# Cairns-Tsallis distribution applied to differences of magnetic field intensity in solar wind

Ewin Sánchez[1,2] and Pedro Vega-Jorquera[2]

[1]Instituto de Investigación Multidisciplinario en Ciencia y Tecnología, Universidad de La Serena, Chile
[2]Departamento de Física, Universidad de La Serena, Chile
**Correspondence:** Ewin Sánchez (esanchez@userena.cl)

**Abstract.** Relevance of the Cairns-Tsallis probability distribution in its application to time series of spatial magnetic field differences is shown. In particular, we explore its ability to explain the data obtained by the Ulysses mission during solar cycles 23 and 24. Our findings reveal that the Cairns-Tsallis density function provides an optimal fit to the data, showing a sensitivity to the small time scale of magnetic field changes. Fit parameters obtained with this model were analyzed, as well as some multifractal indices obtained through corresponding time series analysis. Furthermore, significant discrepancies have been identified between our results and those obtained by other authors, highlighting the appropriateness of the Cairns-Tsallis distribution in capturing the underlying complexity in the data.

## 1 Introduction

To understand the Sun-Planet interaction, it is necessary to study in detail the solar wind dynamics as a means of transport bringing effects of solar origin events to other objects that make up the solar system. Research to date has focused primarily on understanding the solar wind dynamics in the Sun-Earth interaction. The Sun-Earth system is a complex, electrodynamically coupled system, in which nonlinear interactions predominate. Its complex behavior is manifested due to the far from equilibrium state, where nonlinear phenomena and turbulence play a key role in its dynamics. Interplanetary space is full of plasma (Marsch et al., 1982) ejected by the Sun, which drags the magnetic field of solar origin. This frozen magnetic field into the flow is referred to as the Interplanetary Magnetic Field (IMF). Since the article by Coleman (1968), who showed the link between power spectrum of fluctuations in solar wind and the Kolmogorov's phenomenology of a turbulent fluid (Kolmogorov, 1941), researchers have been assessing different aspects of solar wind fluctuations in terms of turbulence (Osman et al. (2012); Li et al. (2011) and references therein). Turbulence is a typical phenomenon of several space plasma systems addressed in a wide range of scales (Bruno and Carbone, 2013). In addition, turbulence in different regions of the Earth's magnetosphere-ionosphere-atmosphere and its relationship with the solar wind turbulence has been widely discussed (see e.g. Echim et al. (2007); Liu et al. (2019)). The effect of turbulence in the solar wind on the turbulent cascade in the magnetosheath has been studied by other authors (see e.g. Rakhmanova et al. (2019) and references therein). Using magnetic

25    field data from CLUSTER II in the plasma sheet, it has been shown that the magnetic field fluctuations have multi-scale characteristics, and that turbulence is intermittent. Intermittency means that fluctuations in energy are not equally distributed (Weygand et al., 2005), or more generally, spatial and/or time physical variables change abruptly. Thus, the high turbulence that characterizes the dynamics of the solar wind reveals intermittent structures associated with current sheets and boundaries between adjacent flux tubes at large scales, as well as differences in

30    intermittency at small scales (see e.g. Wang et al. (2013); Osman et al. (2014) and references therein). Two universal properties of turbulent systems have been proposed: First, within the inertial range the power-law spectrum shows scale invariance, i.e. the same physical description is valid, independent of each measurement scale, and second, intermittency due to non-uniformity in the energy transfer between scales. According to previous studies, space plasmas such as, the solar wind, the magnetosphere and astrophysical systems, show to be highly complex systems,

35    both on a global and small scale. Stochastic fluctuations and coherent structures stand out in their dynamics (see e.g. Bruno and Carbone (2013) and references therein). Of relevance are fluctuations from a spatial and/or temporal point of view. In regions of solar wind and magnetosphere, the magnetic field and velocity fluctuations are characterized by non-Gaussian distributions at small scales (see e.g. Consolini et al. (2009), hereafter CBD2009, and references therein). According to Frisch (1995), intermittency is related to fluctuations in the MHD turbulence

40    framework, which manifest as non-uniformities in dissipative structure distributions. A consequence of this, it is the deviation from Gaussian distribution in the cascade process development (Sorriso-Valvo et al. (2001); Bruno and Carbone (2013) and references therein). In addition to intermittencies, other mechanisms have been proposed as relevant for the solar wind: the mixture of stochastic fluctuations and coherent structures (Tu and Marsch, 1995); the relation between coarse-grained multiscale coherent structures and large-amplitude fluctuations (Chang et al.,

45    2004; Wu and Chang, 2000); the existence, in other space plasmas scenarios, of coherent structures that could be like flux tubes (Tu and Marsch, 1990; Milovanov and Zelenyi, 2000; Borovsky, 2008). Considering the relevance that coarse-grained stochasticity could have in the solar wind, CBD2009 focus their research on the statistics of the magnetic field intensity on a short-time scale, centering on the deviation from Gaussian distribution function in terms of "grained" magnetic structures. Based on subordination process, and using data from Ulysses mission over

50    a period of 6 months (01 October 1997 to 31 March 1998), they constructed a non-Gaussian statistical description of the small-scale temporal differences of magnetic field intensity. The selected period corresponds to the minimum solar activity, ensuring that radial effects on the B field are negligible and that the Alfvénic fluctuations are highly reduced. Authors proposed a new model, the randomized Weibull distribution, which was fitted to both distributions the magnetic field intensity and the small-scale $B$ differences (fluctuations), showing significant discrepancies at the

55    extremes. The author's interpretation focused on the presence of multi-scale heterogeneity in the magnetic field structures of the system. Notwithstanding the authors' arguments to explain the heavy tail of experimental data distributions, we emphasize the need for a new model that perform a better fit on recorded data. Our motivation to write this work was triggered by the optimal fit we found performing the Cairns-Tsallis (CT) distribution on datasets taken from two plots shown in CBD2009, as can be seen in Fig. 1 and Fig.2. We find that our fitting on

60    the extracted data (https://www.automeris.io for details of extraction) are better than achieved by the randomized
Weibull model proposed by the authors.
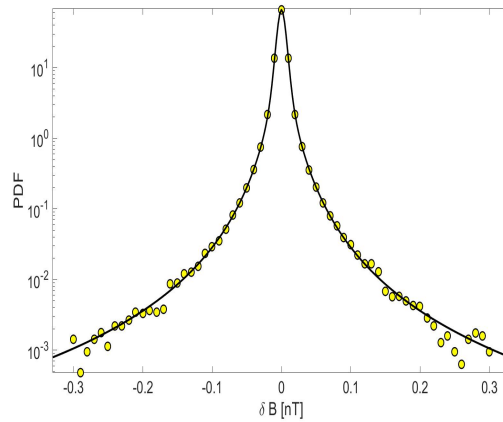


**Figure 1.** Small-scale increments distribution for $\tau = 24$s as shown in CBD2009 (Fig.9). The solid line is the CT PDF fitting.
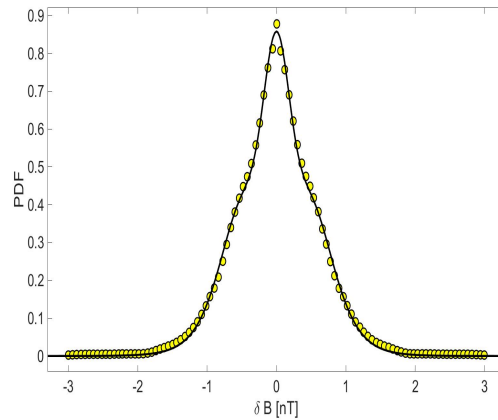


**Figure 2.** Small-scale increments distribution of permutated time-series as shown in CBD2009 (Fig.10). The solid line is the CT PDF fitting.

An adequate statistical description of the magnetic field fluctuations will allow valuable insights into the understanding of the physical processes involved in its dynamics. The above discussions clearly show that a better model

is crucial to understand the complex physical processes involved in the dynamics of the Sun-Earth system. The
purpose of this work is to apply the CT probability density function (PDF) to four data sets linked to solar cycles
23 and 24, as well as performing a multifractal analysis to reinforce the results obtained.

## 2 Procedure and results

### 2.1 The CT distribution

This distribution was introduced in Tribeche et al. (2012) to describe particle velocity distributions in nonthermal
plasmas, capturing both the nonthermality and non-extensivity acting in these environments. It was presented as a
generalization of the Cairns et al. (1995) model, proposing a more physically meaningful approach that better fits
space observations due to flexibility of the nonextensive parameter $q$.

On one side, the Cairns distribution describes non-thermal plasmas, where particles show high energies or ex-
cess of fast particles compared to predictions of a Maxwell-Boltzmann distribution. This distribution modifies the
Maxwellian distribution function by adding an additional term. Non-thermality in plasmas can affect wave propa-
gation, develop turbulence and influence collision processes (Wilson, 1962; Rehman, 2018).

On the other hand, non-extensivity reflects the presence of long-range interactions, strong correlations, and heavy-
tailed probability distributions. The Tsallis non-extensive statistics arise from a generalization of the Boltzmann-
Gibbs entropy presented in Tsallis (1988), which is defined as

$$S_q = k_B \frac{1 - \sum_i p_i^q}{q-1} \tag{1}$$

where $k_B$ is the constant of Boltzmann, $p_i$ is the microstate probability $i$ and $q$ is the no-extensivity parameter.
For $q \rightarrow 1$ this entropy reduces to the Boltzmann entropy. The role of the parameter $q$ in determining the system's
complexity degree has been addressed in some papers (Abe et al., 2004; Yamano, 2004; Virgilio and Murta, 2012).
Application of Tsallis statistics allows a more suitable description of some non-equilibrium systems, capturing the
complexity and non-linear behaviors that cannot be adequately described by classical Boltzmann-Gibbs statistics.
We can observe non-extensivity in some systems, such as plasmas, where interactions between particles do not fall
rapidly with distance, implying a strong and persistent correlation between them. But also, some systems with
fractal or multifractal structure can be non-extensives because some of their properties can vary non-trivially with
scale. Then, the CT PDF becomes a solid model, mixing both the non-extensivity and the non-thermality.

In Tribeche et al. (2012) it was demonstrated that the CT distribution, when applied to non-thermal electrons,
significantly affects the coexistence of rarefactive and compressive solitary waves in plasmas. In Amour et al. (2012)
the authors explored propagation of electron acoustic solitary waves in plasmas with non-thermal electrons. They
have highlighted the sensitivity of solitary wave properties to non-extensivity and non-thermality parameters. Also,
Abid et al. (2016) analyzed the current balance equation for negatively charged dust grains in a non-Maxwellian
plasma, modelled with the CT distribution function. On the other hand, an important work regarding the range of

validity and limitations of the CT distribution was presented in Williams et al. (2013). In that paper the authors reexamined the CT model and found that its validity is restricted to specific ranges of the non-extensivity $q$ and non-thermality $\beta$ parameters. Their study revealed that although the model is useful, it should be applied with caution due to its limitations in certain ranges of its parameters.

100    The 1-D non-extensive non-thermal velocity PDF, which now is known as the CT distribution, is given by

$$p(v_x) = C_{q,\beta}\left(1 + \frac{\beta v_x^4}{v_{th}^4}\right)\left[1 - (q-1)\frac{v_x^2}{v_{th}^2}\right]^{\frac{1}{q-1}}. \tag{2}$$

The constant of normalization, when $-1 < q \leq 1$, is

$$C_{q,\beta} = \frac{\eta}{v_{th}}\frac{\Gamma(\frac{1}{1-q})(1-q)^{5/2}}{\Gamma(\frac{1}{1-q}-\frac{5}{2})[3\beta + (\frac{1}{1-q}-\frac{3}{2})(\frac{1}{1-q}-\frac{5}{2})(1-q)^2]} \tag{3}$$

with $v_{th} = \sqrt{T_e/m_e}$ the electron thermal velocity and $\eta = n_{e0}/\sqrt{2\pi}$. As the nonextensive character of nonthermal
105  electrons increases, a prominence of "shoulders" is observed on respective fit curve and the probability of high-energy states may differ from the extensive nonthermal case. For $\beta = 0$, the well-known Tsallis non-extensive distribution emerges from (2). When $q \to 1$ the Cairns distribution is obtained, and for $\beta = 0$ and $q \to 1$ then we have the Maxwellian distribution.

A similar behavior of interplanetary space magnetic field and solar wind speed at different space/time scales has
110  been found (Burlaga and Viñas, 2004; Matteini et al., 2014) and several statistical studies with some Tsallis-like distributions have been performed. For example, analysis of the magnetic field in the distant heliosphere (Burlaga and Viñas, 2005), or in the heliosheath (Burlaga et al., 2006; Burlaga and Ness, 2009, 2012), or beyond the heliopause (Burlaga and Ness, 2014), or in the local interstellar medium (Burlaga, 2015). Also, solar wind speed fluctuation at 1 AU has been addressed by Burlaga and Viñas (2004).

115  Even though the CT distribution was originally applied to velocity distributions, we can extrapolate its application to differences $\delta B$ of magnetic field intensity $B$ data, given the connection between charged particle dynamics and magnetic field fluctuations in the plasma. Certainly, for consistency with our proposal, we need to make the following substitutions in (2): $v \longmapsto \delta B$, the differences of magnetic field intensity, $v_{th} \longmapsto B_*$, some constant that has same dimensions as $B$ (it corresponds to the medium width of the PDF) and $\eta \longmapsto \eta_*$. Extrapolation of CT distribution to
120  other systems is nothing new. Application to the dipole-type Hamiltonian mean-field model was presented recently in Sánchez and Atenas (2023). Magnetic field intensity is directly influenced by the dynamics of charged particles in the plasma, which follow velocity distributions that can be characterized by the CT model. Therefore, by modeling magnetic field differences, we are indirectly capturing the underlying physics that governs particle velocity distributions. This relationship would allow that flexibility and accuracy of the CT distribution describing non-extensivity
125  and non-thermality in velocity distributions, to be applied to magnetic field intensity distributions as well, providing a consistent and robust description of plasma properties. In the solar wind environment, such as that observed by the Ulysses mission, charged particles, mainly protons and electrons, constantly interact with the interplanetary

magnetic field. These interactions produce fluctuations, generally in small-scales, on the magnetic field intensity
that may reflect the velocity distribution of the underlying particles. The benefit of the new proposed CT model is
130    improving poor fits usually obtained with different distribution functions in several space plasma environments.

## 2.2 CT PDF fitting

The time series analysis using differences is a common technique in various disciplines due to its advantages in
data management and extraction of relevant information. This technique, known as differencing, has important
applications in economics, finance, physics, and other areas and results from computing the differences between
135    consecutive observations in the time series. Here, $\delta B_i$ is defined as the difference in the magnetic field intensity $B$ in
a small time interval $\tau$, is worth to say, $\delta B_i = B_{i+\tau} - B_i$. This approach on small time scales allows us to detect local
changes in the magnetic field, which can be indicators of turbulent and intermittent phenomena. Intermittency in
plasma turbulence manifests itself as large and sporadic fluctuations in, for example, the magnetic field, which are
most evident in small-scale differences. The probability distributions of small-scale differences $\delta B_i$ typically show
140    non-Gaussian and leptokurtic (fat-tailed) shapes, which are key characteristics of intermittent MHD turbulence. By
studying $\delta B_i$ with small $\tau$, we observe the local change rates of the magnetic field, allowing us to identify local
variations in $B$, which could be indicative of turbulence.

The resulting time series $\delta B = \{\delta B_1, ..., \delta B_n\}$ for each dataset that we selected (which we will detail later) is highly
non-stationary, as reflected in the autocorrelation function plot shown in Fig. 3 for the case of the dataset taken
145    during 1996-1997, whose behavior also reflects the dynamics for the rest of selected datasets.
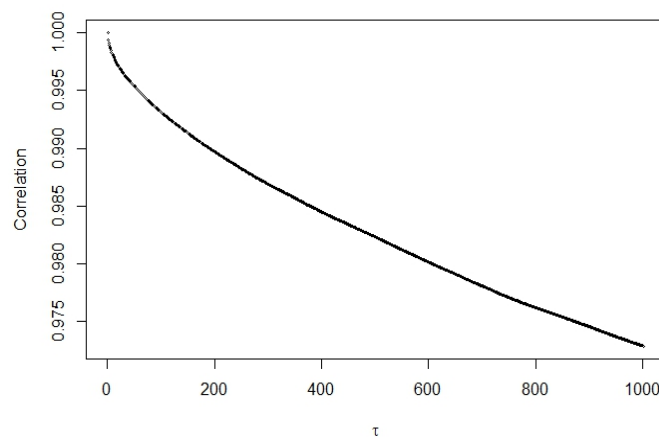


**Figure 3.** Autocorrelation function for the 1996-1997 intensity magnetic field dataset.

Given our findings when CT PDF was applied to the distribution of magnetic field differences from the CBD2009 paper, we have gone further. We have analyzed 4 datasets taken from the Ulysses mission database, which include periods from October 01 to March 10 between the years 1996-1997, 1997-1998, 2000-2001 and 2001-2002. This choice was based on the maximums and minimums observed between the beginning of SC23 and the beginning of SC24, according to the sunspot activity on the Sun shown in Fig. 4 (data taken from WDC-SILSO, Royal Observatory of Belgium, Brussels). Ulysses covered a time span from 1990-10-25 to 2009-06-30, recording magnetic field magnitude data from the Vector Helium Magnetometer (for more details see Balogh et al. (1992)). Here, we are interested in knowing if the one-dimensional CT PDF is capable of characterizing the chosen periods of maximum and minimum activity through the respective fit parameters.
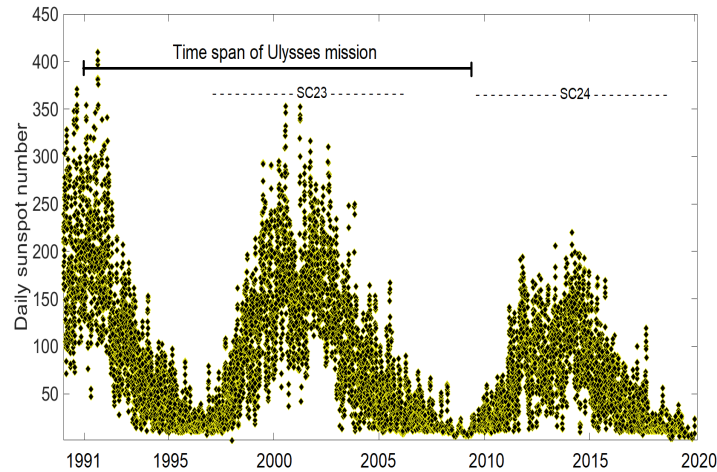


**Figure 4.** Daily sunspot number, from begin of 1990 to the end of 2019.

We have taken the data without filtering and then analyzing them with the Matlab Curve Fitting Toolbox. After several tests it was found that Eq.(2) for $-1 < q \leq 1$ could fit the data, unlike the form for $q \geq 1$ (shown in the Tribeche et al. (2012) paper). We have used a robust method, fitting the CT PDF to each dataset using bisquare weights, with restrictions $0 < q < 1$, $\beta > 0$, $B_* > 0$ and $\eta_* > 0$. In each data set, the fitting of the CT PDF was tested starting from $\tau = 1$s, repeating the fitting for $\tau = 2, 3, ...$ (seconds) when it had not converged. Then, we found the optimal fit when $\tau = 1$s for the 2000-2001 and 2001-2002 datasets and, on the other hand, when $\tau = 5$s and $\tau = 7$s for datasets 1996-1997 and 1997-1998, respectively. Curve fitting results to each dataset are depicted in Fig. 5.
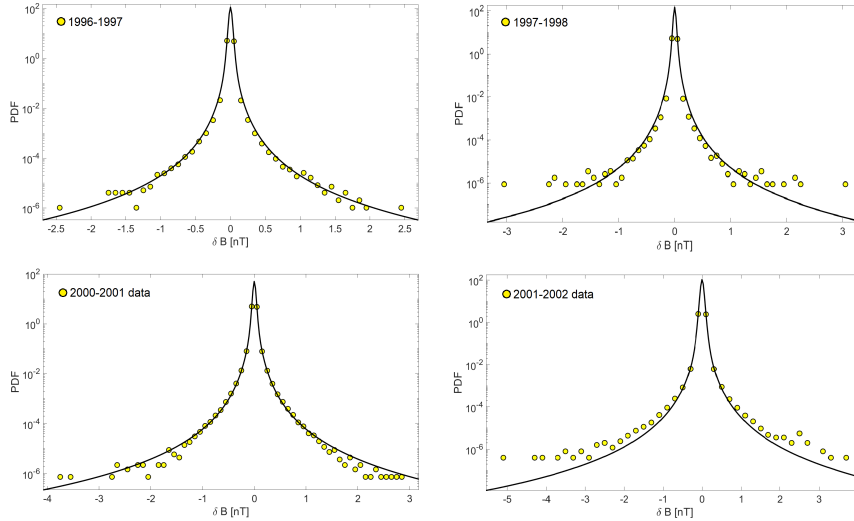
**Figure 5.** CT PDF fitting on all datasets.

A summary of results can be seen in Table 1, where relevant fit parameters $q$, $\beta$ and $B_*$ are shown. The minimum lag ($\tau$) from which optimal fitting of (2) was reached can also be seen for each case. The average for $q$ obtained from fit values shown in Table 1 is $\bar{q} = 0.7628$.

165     The above results show that non-thermal effects are present in the system even for small values of $\beta$. These non-thermal effects are due to presence of superthermal particles in the plasma, which are modeled by the parameter $\beta$. We have checked the non-thermality influence calculating $(1/n)\sum_i[1 + \beta(\delta B_i/B_*)^4]$ (the average value of Cairns factor) for each dataset (see Table 1). It has been stated that the non-extensivity and non-thermality mixture produces significant effects when $0 \leq \beta < 0.25$. Within this specific range, both non-extensivity and non-thermality

170     affect plasma properties, such as the propagation of solitary waves. Some authors have found that nature of electron-acoustic solitary waves and double layers critically depend on the entropic index $q$ and the non-thermal parameter $\beta$, even when values of this latter parameter are very small (Bala et al., 2021). As $\beta$ approaches 0.25, non-extensive effects tend to disappear, leaving only non-thermal effects (Farooq et al., 2018). Such restrictions, both for $q$ and $\beta$, were also announced earlier in Williams et al. (2013). Here, our results satisfy the condition $0.6 < q \leq 1$ and

175     $\beta \leq (2q-1)/4$ shown in the latter mentioned paper.

    According to our findings, it seems that CT PDF does not recognize the calm and intense conditions under which the data were recorded. In many cases the behavior of $q$ is different. For example, when storms are observed in the magnetosphere or shocks in the plasma of solar wind, values of non-extensivity parameter $q$ tend to increase during periods of maximum activity, compared to periods of minimum activity (Pavlos et al., 2012, 2015). Then, could the

180     system in some cases be represented by a similar $q$ parameter in both states?. To analyze the results in more depth, respect to this issue, we have used a different perspective, performing a multifractal analysis.

| Dataset | q | $\beta$ | $B_*$ | $\tau$ | $\overline{1+\beta(\delta B_i/B_*)^4}$ |
|---|---|---|---|---|---|
| 1996-1997 | 0.7544 | 9.67E-04 | 0.01601 | 5 | 2.09591 |
| 1997-1998 | 0.7784 | 1.29E-03 | 0.01518 | 7 | 2.15057 |
| 2000-2001 | 0.7498 | 2.06E-03 | 0.01935 | 1 | 4.96542 |
| 2001-2002 | 0.7687 | 4.07E-04 | 0.02847 | 1 | 1.33784 |

**Table 1.** Relevant results obtained from the CT PDF fitting.

## 2.3 The Multifractal Detrended Fluctuation Analysis

Since fluctuations of interplanetary magnetic field intensity show non-Gaussian distributions, then, an underlying multifractal structure could exist. Multifractality in time series refers to the presence of multiple fluctuation scales in a time series, which implies a more complex variability than that described by monofractality, where the time series has a single self-similarity structure and can be characterized by a single Hurst exponent $H$ (Hurst, 1951). There are several methods of multifractal analysis, such as the Wavelet Transform Modulus Maxima Method (WTMM), the Multifractal Detrended Cross-Correlation Analysis (MF-DCCA) and the Detrended Fluctuation Analysis (DFA), of which we have performed the latter. The Multifractal Detrended Fluctuation Analysis (MFDFA) is a technique used to detect and analyze multifractality in time series (see Appendix A).

We have performed the MFDFA analysis using the Ihlen (2024) Matlab code, previously customized. A polynomial first order was choosen for the detrending, with a minimum size segment equal to 512 (maximum size 524288). Fig. 6 shows the results of the generalized Hurst exponent as a function of the $Q$ moment and the singularity spectrum as a function of the Hölder exponent $\alpha$ for different data sets. Fig. 6a: (1996-1997); Fig. 6b: (1997-1998); Fig. 6c: (2000-2001); Fig. 6d: (2001-2002).
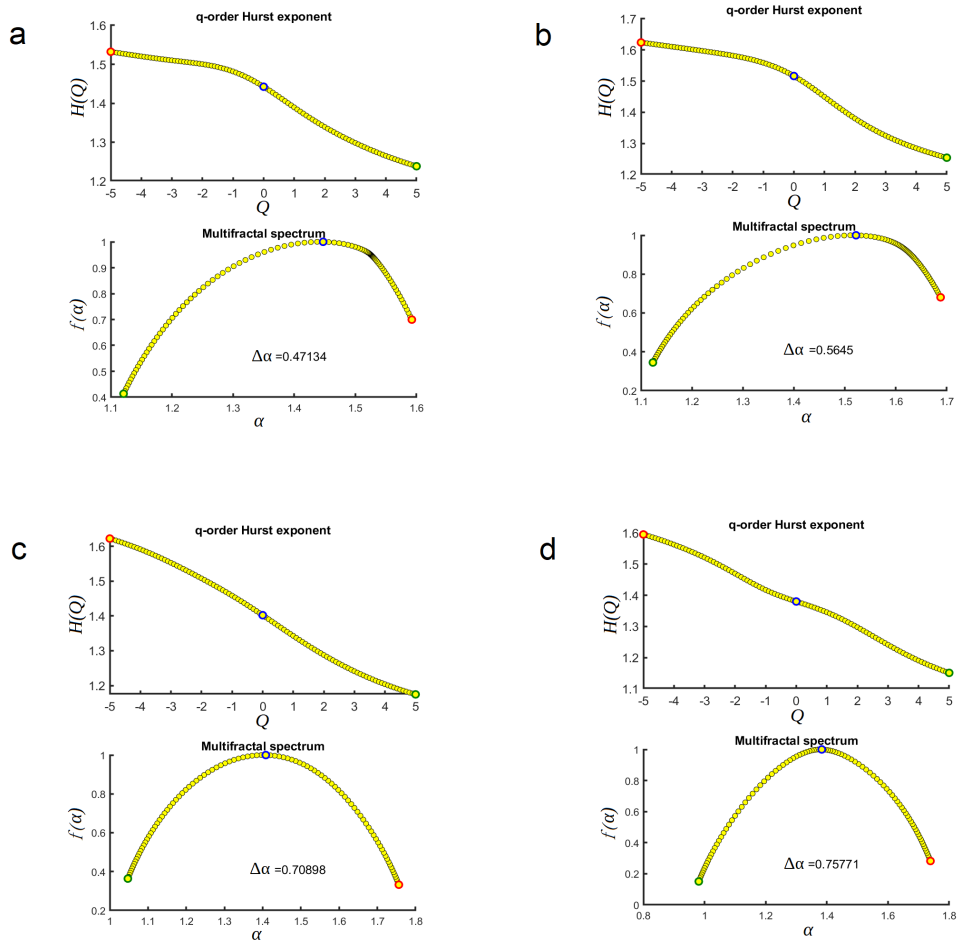
**Figure 6.** Multifractal analysis for datasets (a) 1996-1997, (b) 1997-1998, (c) 2000-2001 and (d) 2001-2002.

The generalized Hurst exponent $H(Q)$ plot shows how the self-similarity of the time series changes when different fluctuation aspects are observed. For positive values of $Q$, $H(Q)$ describes the scaling behaviour of time series segments with large fluctuations, while, for negative values it does with small fluctuations. We can notice that the range of values of $H(Q)$ are similar in all datasets. This might happen because the Hurst exponent $H(Q)$ measures memory and persistence in time series, providing information about the trend of the data and general patterns of behaviour in the dynamics of the system, but it does not specify which are the specific structures that generate the observed persistence (or antipersistence), nor how the correlations are distributed on different time scales. Similarly, the non-extensive parameter $q$ tells us about the deviation from the Boltzmann-Gibbs statistic and the non-extensive nature of the probability distribution in the data, but it does not specify the temporal or spatial distribution of the long-range interactions or the particular structures within the system.

| Dataset | $H(Q)$ minimum | $H(Q)$ maximum | $\Delta\alpha$ |
|---------|----------------|----------------|----------------|
| 1996-1997 | 1.23 | 1.53 | 0.471 |
| 1997-1998 | 1.25 | 1.62 | 0.564 |
| 2000-2001 | 1.18 | 1.62 | 0.708 |
| 2001-2002 | 1.15 | 1.59 | 0.757 |

**Table 2.** Relevant multifractal indexes obtained through the MFDFA analysis.

On the other hand, the $f(\alpha)$ plot is useful for understanding the diversity of local behaviours (singularities) in the system, reflecting its complexity and hierarchical structure (Halsey et al., 1986; Ott, 2002). In particular, we are interested in the width $\Delta\alpha$ of the spectrum, defined as the difference $\alpha^{max} - \alpha^{min}$ between the maximum and minimum values of $\alpha$, which indicates the variation amplitude of singularities in the system. We can observe the

210   largest spectral width $\Delta\alpha$ for datasets recorded on maximum solar activity (2000-2001 and 2001-2002). This indicates a greater singularity diversity in the corresponding time series and could be an indication of a greater intermittency during the respective periods considered. That is, considering that turbulence is generally intermittent, we can conclude that it critically depends on solar activity. Yordanova et al. (2009) showed that the intermittency level depends on the different solar winds flows, which, in turn, depends on the sources of origin. From here, we can

215   assume that the highest level of intermittency occurs during periods of highest solar activity, so we would expect an increase in the spectral singularity range. However, further analyses are necessary to confirm this (see, e.g., Macek (2007)). We also observe the branches of the $f(\alpha)$ curve, which tells us about the distribution of singularities in the system, allowing us to know what type of singularities (weaker or stronger) are more or less prevalent. In Fig. 6 we can see a shorter right branch for the 1996-1997 and 1997-1998 datasets, indicating a prominent presence of

220   singularities with a higher exponent $\alpha$, suggesting a greater density of regions with a lower singularity strength. A summary with relevant multifractal indexes are shown in Table 2.

Then, the spectrum of singularities gives us more precise information, by providing a more detailed perspective of irregularities diversity and dynamics complexity of the underlying processes. To illustrate the mentioned above, we can also look at literature of other complex systems. For example, in the neurological signal analysis we can find

225   that $H(Q)$ and $f(\alpha)$ provide different insights into the results. More specifically, electroencephalographic signals of normal and epileptic patients were analyzed, on the one hand, through the spectrum of singularities (He et al., 2007) and on the other hand, through the generalized Hurst exponents (Lahmiri, 2018), where the first of those provides a more detailed understanding about complexity and variety in the signals. Different interpretations provided by each of these multifractal indicators can also be seen in Sorriso-Valvo et al. (2017), where proton density fluctuations in

230   the solar wind were evaluated in different ranges of scales.

## 3   Final remarks

We have presented the CT distribution as a suitable and effective model to explain data of small-scale magnetic field intensity differences obtained from data recorded by the Ulysses mission. We have analysed 4 datasets: 1996-1997; 1997-1998; 2000-2001 and 2001-2002, so that they coincide with minimum and maximum solar activity periods

235   (among which we can find the period selected by CBD2009). We have found that small-scale differences $\delta B_i$ show significant dynamics even over very short time intervals. We have observed that for periods of high solar activity (represented by the 2000-2001 and 2001-2002 datasets) the CT PDF is able to adequately capture the dynamics from $\tau = 1$s, explaining accurately the distribution of local changes in the magnetic field. On the other hand, during periods of minimum solar activity (represented by the datasets 1996-1997 and 1997-1998) the CT PDF is properly

240   fitted from $\tau = 5$s and $\tau = 7$s. This indicates that, in this second case, longer time intervals are required so that the CT PDF captures the dynamical behaviour of system through the distribution of differences $\delta B_i$. The mentioned above suggests that there could be different temporal responses to the physical conditions of the environment. The CT PDF fitting at $\tau = 1$s suggests that intermittency and non-Gaussian fluctuations occur really quickly, and these are immediately reflected by the CT PDF, unlike to minimal activity periods, where the most significant fluctuations

245   and coherent structures within the reach of CT PDF take longer to develop. Then, the observed differences in the time scales $\tau$ for the PDF CT fitting would suggest that the characteristic scales of plasma dynamics change with solar activity.

The $1 + \beta(\delta B/B_*)^4$ factor of the CT distribution, which we have considered, introduces a correction that affects the overall shape of the distribution. Although $\beta$ is small in all the analyzed cases, the performed fittings show that

250   this term still has an impact on the shape of the distribution, especially in the tails. The Tsallis distribution, without the factor above, could not properly capture these non-thermal effects on its own. Our results show that the system experiences significant non-thermal and non-extensivity effects, where $\beta \ll 1$ and $0.75 < q < 0.78$.

On the other hand, we performed a multifractal analysis to understand better the fit values of parameter $q$ obtained through the CT PDF. We can notice that both values $H(Q)$, provided by the MFDFA analysis, and $q$, obtained

255   through the CT PDF, are similar for all datasets (see Table 1 and Table 2), possibly due to these parameters do not fully capture details of the complexity given by the underlying dynamic processes. The similar range of $H(Q)$ obtained in both datasets indicates that data from solar maximum and minimum periods have a similar correlation structure, showing a strong persistence over time. Also, in all cases the system keeps a strong non-equilibrium state, where $\bar{q} = 0.7628$ (see Table 1) is verified. The multifractality and diversity of these processes have been best

260   reflected by means of singularity spectrum width, which has revealed significant differences between the periods of maximum and minimum solar activity, pointing out significant variations in the complexity and diversity of the underlying processes that are not captured by $H(Q)$ or $q$. In specific, the greater spectral width $\Delta\alpha = 0.708$ and $\Delta\alpha = 0.755$ for datasets corresponding to the maximum activity period, compared to the spectral width $\Delta\alpha = 0.471$ and $\Delta\alpha = 0.564$ datasets corresponding to the minimum activity period, indicates a greater diversity of dynamical

265 processes and complexity in the structure of the time series during periods of high solar activity. Thus, it is possible
that both periods (maximum and minimum solar activity) share similar fundamental features in terms of solar wind
dynamics, such as magnetohydrodynamic (MHD) turbulence, resulting in values of $q$ and in range of $H(Q)$ similar
in both cases, so these could be capturing some inherent property of these processes, independent of the intensity of
solar activity. On the other hand, singularity spectrum indicates the existence of different environmental conditions
270 or external perturbations for both periods.

Therefore, the choice of the CT distribution to model differences of the magnetic field intensity in the solar wind is
an extrapolation that takes advantage of the relationship between particle dynamics and magnetic field properties.
This provides a solid tool to analyze and describe the complex interactions and distributions in the solar wind
plasma, offering a more complete and precise perspective on its behavior than those presented by other authors.

275 *Data availability.* The raw data required to reproduce the above findings are available from https://cdaweb.gsfc.nasa.gov

## Appendix A: The Multifractal Detrended Fluctuation Analysis

Let us consider the $x_l$ time series from which we generate another new time series (Kantelhardt et al., 2002)

$$Y(j) = \sum_{l=1}^{j} [x_l - \langle x \rangle] \tag{A1}$$

where $x_l$ are the original points of time series and $\langle x \rangle$ is the mean value. We divide this into segments of size $s$.
280 A polynomial of order $m$ is fitted within each $v$-th segment,

$$y_v(i) = \sum_{k=0}^{m} C_k i^{m-k}, \tag{A2}$$

where $C_k$ are the polynomial coefficients. To eliminate local trends, the average amplitude of local fluctuations in
non-overlapping segments is calculated through the root mean square (RMS) variation.

$$F(s,v) = \sqrt{\frac{1}{s} \sum_{i=1}^{s} \{Y[(v-1)s+i] - y_v(i)\}^2}. \tag{A3}$$

285 Then, the global scaling function is calculated for multiple segment sizes $s$, i.e.,

$$F(s) = \sqrt{\frac{1}{N_s} \sum_{v=1}^{N_s} F^2(s,v)} \tag{A4}$$

where $N_s$ is the segments number of size $s$.

To capture multifractality, we extend the DFA analysis to a $Q$-order moment analysis through

$$F_Q(s) = \left\{ \frac{1}{N_s} \sum_{v=1}^{N_s} [F(s,v)]^Q \right\}^{\frac{1}{Q}}. \tag{A5}$$

For $Q = 0$ we have

$$F_0(s) = \exp\left(\frac{1}{2N_s}\sum_{v=1}^{N_s}\ln[F^2(s,v)]\right). \tag{A6}$$

The generalized Hurst exponents of order $Q$ are obtained from the slope of the log-log relationship between $F_Q(s)$ and $s$, which means that

$$H(Q) = \frac{d\ln F_Q(s)}{d\ln s}. \tag{A7}$$

From this, the singularity spectrum $f(\alpha)$ is obtained through the following transformation

$$\tau(Q) = QH(Q) - 1 \tag{A8}$$

and subsequently,

$$\alpha = \frac{d\tau(Q)}{dQ}, \quad f(\alpha) = Q\alpha - \tau(Q), \tag{A9}$$

where $f(\alpha)$ inform about the fractal dimension of the subsets with singularity strength $\alpha$, which is known as the generalized Hölder exponent and it is a measure of the local singularity.

*Author contributions.* P.V.: Conceptualization, Writing, Analysis, Review and Editing. E.S.: Writing, Original Draft, Software, Analysis, Review and Editing

*Competing interests.* The authors declare no competing interest.

Nonlinear Processes
in Geophysics
Discussions

Open Access

EGU

# References

305    Abe, S., Landsberg, P. T., Plastino, A. R., and Yamano, T.: Nonadditive statistical measure of complexity and values of the entropic index q, https://doi.org/arXiv:cond-mat/0402217v1, 2004.

Abid, A. A., Khan, M. Z., Yap, S. L., Terças, H., and Mahmood, S.: Dust charging processes with a Cairns-Tsallis distribution function with negative ions, Phys. Plasmas, 23, 013 706, 2016.

Amour, R., Tribeche, M., and Shukla, P. K.: Electron acoustic solitary waves in a plasma with nonthermal electrons featuring

310    Tsallis distribution, Astrophys Space Sci, 338, 287–294, 2012.

Bala, P., Kaur, A., and Kaur, K.: Arbitrary amplitude electron-acoustic solitons and double layers with Cairns–Tsallis-distributed hot electrons, Pramana - J Phys, 95, 20, https://doi.org/10.1007/s12043-020-02060-2, 2021.

Balogh, A., Beek, T. J., Forsyth, R. J., Hedgecock, F. C., Marquedant, R. J., Smith, E. J., Southwood, D. J., and Tsurutani, B. T.: The magnetic field investigation on the ULYSSES mission - Instrumentation and preliminary scientific results,

315    Astronomy and Astrophysics Supplement Series, 92, 221–236, 1992.

Borovsky, J. E.: Flux tube texture of the solar wind: Strands of the magnetic carpet at 1 AU?, Journal of Geophysical Research, 113, A08 110, https://doi.org/https://doi.org/10.1029/2007JA012684, 2008.

Bruno, R. and Carbone, V.: The solar wind as a turbulent laboratory, Living Reviews in Solar Physics, 10, https://doi.org/https://doi.org/10.12942/lrsp-2013-2, 2013.

320    Burlaga, L. F.: Voyager observations of the magnetic field in the heliosheath and the local interstellar medium, Journal of Physics: Conference Series, 642, 012 003, https://doi.org/10.1088/1742-6596/642/1/012003, 2015.

Burlaga, L. F. and Ness, N. F.: Compressible turbulence observed in the heliosheath by Voyager 2, Astrophys. J., 703, 311–324, 2009.

Burlaga, L. F. and Ness, N. F.: Magnetic field fluctuations observed in the heliosheath by Voyager 1 at 114 2 AU during 2010,

325    J. Geophys. Res., 117, A10 107, https://doi.org/10.1029/2012JA017894, 2012.

Burlaga, L. F. and Ness, N. F.: Interstellar magnetic fields observed by voyager 1 beyond the heliopause, The Astrophysical Journal Letters, 795, L19., 2014.

Burlaga, L. F. and Viñas, A. F.: Multiscale structure of the magnetic field and speed at 1 AU during the declining phase of solar cycle described by a generalized Tsallis probability distribution function, A12107, 109, A12 107,

330    https://doi.org/10.1029/2004JA010763, 2004.

Burlaga, L. F. and Viñas, A. F.: Triangle for the entropic index q of nonextensive statistical mechanics observed by Voyager 1 in the distant heliosphere, Physica A, 356, 375–384, https://doi.org/10.1016/j.physa.2005.06.065, 2005.

Burlaga, L. F., Ness, N. F., and Acuña, M. H.: Multiscale structure of magnetic fields in the heliosheath, J. Geophys. Res., 111, A09 112, https://doi.org/10.1029/2006JA011850, 2006.

335    Cairns, R., Mamum, A., Bingham, R., Bostrom, R., Dendy, R., Nairn, C., and Shukla, P.: Electrostatic solitary structures in non-thermal plasmas, Geophys. Res. Lett., 22, 2709, 1995.

Chang, T., Tam, S. W. Y., and Wu, C. C.: Complexity induced anisotropic bimodal intermittent turbulence in space plasmas, Phys. Plasmas, 11, 1287–1299, 2004.

Coleman, P. J.: Turbulence, Viscosity, and Dissipation in the Solar-Wind Plasma, ApJ, 153, 371, 1968.

Nonlinear Processes
in Geophysics
Discussions

340    Consolini, G., Bavassano, B., and Michelis, P. D.: A probabilistic approach to heterogeneity in space plasmas: the case of magnetic field intensity in solar wind, Nonlin. Processes Geophys., 16, 265 273, 2009.

Echim, M. M., Lamy, H., and Chang, T.: Multi-point observations of intermittency in the cusp regions, Nonlin. Processes Geophys., 14, 525–534, 2007.

Farooq, M., Mushtaq, A., and Shamir, M.: Analysis of Cairns-Tsallis distribution for oblique drift solitary waves in a rotating

345    electron-positron-ion magneto-plasma, Physics of Plasmas, 25, 122 110, https://doi.org/10.1063/1.5055757, 2018.

Frisch, U.: Turbulence: The Legacy of A. N. Kolmogorov, Cambridge University Press, Cambridge, 1995.

Halsey, T., Jensen, M., Kadanoff, L., Procaccia, I., and Shraiman, B.: Fractal measures and their singularities: The characterization of strange sets, Phys. Rev. A, 33, 1141–1151, 1986.

He, A., Yang, X., Yang, X., and Ning, X.: Multifractal analysis of epilepsy in electroencephalogram, IEEE/ICME international

350    conference on Complex Medical Engineering, pp. 23–27, 2007.

Hurst, H. E.: Long-term storage capacity of reservoirs, Trans. Am. Soc. Civil Eng., 116, 770–799, 1951.

Ihlen, E.: Multifractal detrended fluctuation analyses, https://www.mathworks.com/matlabcentral/fileexchange/ 38262-multifractal-detrended-fluctuation-analyses, 2024.

Kantelhardt, J. W., Zschiegner, S. A., Koscielny-Bunde, E., Havlin, S., Bunde, A., and Stanley, H. E.: Multifractal detrended

355    fluctuation analysis of nonstationary time series, Physica A, 316, 87–114, 2002.

Kolmogorov, A.: The Local Structure of Turbulence in Incompressible Viscous Fluid for Very Large Reynolds' Numbers, Akademiia Nauk SSSR Doklady, 30, 301–305, 1941.

Lahmiri, S.: Generalized Hurst exponent estimates differentiate EEG signals of healthy and epileptic patients, Physica A, 490, 378–385, 2018.

360    Li, G., Miao, B., Hu, Q., and Qin, G.: Effect of Current Sheets on the Solar Wind Magnetic Field Power Spectrum from the Ulysses Observation: From Kraichnan to Kolmogorov Scaling, Physical Review Letters, 106, 125 001, https://doi.org/10.1103/PhysRevLett.106.125001, 2011.

Liu, Y. Y., Fu, H. S., Liu, C. M., Wang, Z., Escoubet, P., Hwang, K. J., Burch, J. L., and Giles, B. L.: Parallel Electron Heating by Tangential Discontinuity in the Turbulent Magnetosheath, Astrophys. J. Lett., 877, L16, https://doi.org/10.3847/2041-

365    8213/ab1fe6, 2019.

Macek, W. M.: Multifractality and intermittency in the solar wind, Nonlin. Processes Geophys., 14, 695–700, 2007.

Marsch, E., Muhlhauser, K. H., Schwenn, R., Rosenbauer, H., Pilipp, W., and Neubauer, F.: Solar wind protons: Threedimensional velocity distributions and derived plasma parameters measured between 0.3 and 1 au, J. Geophys. Res. Space Phys., 87, 52–72, https://doi.org/10.1029/ja087ia01p00052, 1982.

370    Matteini, L., Horbury, T. S., Neugebauer, M., and Goldstein, B. E.: Dependence of solar wind speed on the local magnetic field orientation: Role of Alfvénic fluctuations, Geophys. Res. Lett., 41, 259–265, https://doi.org/10.1002/2013GL058482, 2014.

Milovanov, A. V. and Zelenyi, L. M.: Functional background of the Tsallis entropy: coarse-grained systems and kappa distribution functions, Nonlin. Processes Geophys., 7, 211–221, 2000.

375    Osman, K. T., Matthaeus, W. H., Hnat, B., and Chapman, S. C.: Kinetic Signatures and Intermittent Turbulence in the Solar Wind Plasma, Physical Review Letters, 108, 261 103, https://doi.org/10.1103/PhysRevLett.108.261103, 2012.

Osman, K. T., Matthaeus, W. H., Gosling, J. T., Greco, A., Servidio, S., and et al., B. H.: Magnetic reconnection and intermittent turbulence in the solar wind, Physical Review Letters, 112, 215 002, https://doi.org/10.1103/PhysRevLett.112.215002, 2014.

380   Ott, E.: Chaos in Dynamical Systems, chap. Multifractals, Cambridge University Press, 2002.

Pavlos, G. P., Karakatsanis, L. P., Xenakis, M. N., Sarafopoulos, D., and Pavlos, E. G.: Tsallis statistics and magnetospheric self-organization, Physica A, 391, 3069–3080, 2012.

Pavlos, G. P., Iliopoulos, A. C., Zastenker, G. N., Zelenyi, L. M., Karakatsanis, L. P., Riazantseva, M. O., Xenakis, M. N., and Pavlos, E. G.: Tsallis nonextensive statistics and solar wind plasma complexity, Physica A, 422, 113–135, 2015.

385   Rakhmanova, L. S., Riazantseva, M. O., Zastenker, G. N., Yermolaeva, Y. I., Lodkina, I. G., and Chesalin, L. S.: Turbulent Cascade in the Magnetosheath Affected by the Solar Wind's Plasma Turbulence, Cosmic Research, 57, 443–450, 2019.

Rehman, U.: Resistive drift instabilities for thermal and non-thermal electron distributions in electron-ion plasma, Heliyon, 4, e01 096, https://doi.org/10.1016/j.heliyon.2018.e01096, 2018.

Sánchez, E. and Atenas, B.: Application of Cairns-Tsallis distribution to the dipole-type Hamiltonian mean-field model, Phys.

390   Rev. E, 108, 044 123, https://doi.org/10.1103/PhysRevE.108.044123, 2023.

Sorriso-Valvo, L., Carbone, V., Giuliani, P., Veltri, P., Bruno, R., Antoni, V., and Martines, E.: Intermittency in plasma turbulence, Planetary and Space Science, 49, 1193–1200, 2001.

Sorriso-Valvo, L., Carbone, F., Leonardis, E., Chen, C. H. K., Šafránková, J., and Němeček, Z.: Multifractal analysis of high resolution solar wind proton density measurements, Adv. Space Res., 59, 1642–1651, 2017.

395   Tribeche, M., Amour, R., and Shukla, P. K.: Ion acoustic solitary waves in a plasma with nonthermal electrons featuring Tsallis distribution, Phys. Rev. E, 85, 037 401, 2012.

Tsallis, C.: Possible generalization of Boltzmann-Gibbs statistics, J. Stat. Phys., 52, 479, 1988.

Tu, C. Y. and Marsch, E.: Evidence for a background spectrum of solar wind turbulence in the inner heliosphere, J. Geophys. Res., 95, 4337–4341, 1990.

400   Tu, C. Y. and Marsch, E.: MHD structures, waves and turbulence in the solar wind: Observations and theories, Space Sci. Rev., 73, 1–210, https://doi.org/10.1007/BF00748891, 1995.

Virgilio, E. and Murta, O.: Evaluation of physiologic complexity in time series using generalized sample entropy and surrogate data analysis, Chaos, 22, 043 105, 2012.

Wang, X., Tu, C., He, J., Marsch, E., and Wang, L.: On Intermittent Turbulence Heating of the Solar Wind: Differences between

405   tangential and rotational discontinuities, The Astrophysical Journal Letters, 772, L14, https://doi.org/10.1088/2041-8205/, 2013.

Weygand, J. M., Kivelson, M., and et al., K. K.: Plasma sheet turbulence observed by Cluster II, J. Geophys. Res., 110, A01 205, https://doi.org/10.1029/2004JA010581, 2005.

Williams, G., Kourakis, I., Verheest, F., and Hellberg, M. A.: Re-examining the Cairns-Tsallis model for ion acoustic solitons,

410   Phys. Rev. E, 88, 023 103, 2013.

Wilson, R.: The spectroscopy on non-thermal plasmas, J. Quant. Spectrosc. Radiat. Transfer, 2, 477–484, https://doi.org/10.1016/0022-4073(62)90033-X, 1962.

Wu, C. C. and Chang, T.: 2D MHD simulation of the emergence and merging of coherent structures, Geophys. Res. Lett., 27, 863–866, 2000.

415    Yamano, T.: A statistical measure of complexity with nonextensive entropy, Physica A, 340, 131–137, 2004.

Yordanova, E., Balogh, A., Noullez, A., and von Steiger, R.: Turbulence and intermittency in the heliospheric magnetic field
    in fast and slow solar wind, J. Geophys. Res., 114, A08 101, https://doi.org/10.1029/2009JA014067, 2009.